DESIGN AND TEST OF A NATURAL LAMINAR FLOW/ LARGE REYNOLDS NUMBER AIRFOIL WITH A HIGH DESIGN CRUISE LIFT COEFFICIENT

C. E. Kolesar
Boeing Military Airplane Company
Seattle, Washington

ABSTRACT

This paper reports on a Boeing aerodynamic research activity to design an airfoil for a large airplane capable of very long endurance times at a relatively low Mach number of 0.22. Airplane mission objectives and design optimization resulted in requirements for a very high design lift coefficient (C_l) and a large amount of laminar flow at high Reynolds number to increase the lift/drag ratio and reduce the loiter lift coefficient. Natural laminar flow was selected instead of distributed mechanical suction due to technology maturity differences when the study was performed. A design C_l of 1.5 was identified as the highest which could be achieved with a large extent of laminar flow.

A single element airfoil was designed entirely through a "synthesis" or inverse design process. This process utilized Boeing-developed inverse boundary-layer solution and inverse airfoil design computer codes to create an airfoil section that would achieve the performance goals and have reasonable off-design performance. This airfoil was designed to meet several criteria in addition to a 1.4 design C_l: a maximum C_l of 2.0, laminar flow on the lower surface from leading edge (L.E.) to trailing edge (T.E.) and laminar flow on the upper surface from L.E. to 0.30c followed by a forced transition. The design process and results, including airfoil shape, pressure distributions, and aerodynamic characteristics are presented in this paper.

A two-dimensional (2-D) wind tunnel model was constructed and subsequently tested in the 3 x 7.5 ft NASA Langley Low Turbulence Pressure Tunnel which enabled testing at the full scale design Reynolds number (RN) of 14×10^6. Model instrumentation included 53 static pressure orifices on the upper and lower surfaces at one spanwise station and a series of flush mounted hot-film gages used as boundary-layer laminar-to-turbulent transition detection devices. A comparison is made between theoretical and measured results to establish accuracy and quality of the airfoil design technique for the high lift/natural laminar-flow application.

INTRODUCTION

Boeing has been involved in the development of long endurance vehicles for many years. Design studies for a Continuous Patrol Aircraft (CPA) initiated in 1981 presented some unique challenges for the aerodynamic wing designer. The aircraft shown in Figure 1, was very large and was to be capable of enduring at low altitude for several days. The wing operated at relatively high Reynolds Number. A review of the literature indicated that while development work had been done for high lift/low drag sections at Reynolds numbers $\leq 1 \times 10^6$, there had been no airfoil sections designed suitable for the operating requirements of the CPA. Therefore, a parallel research and development study was initiated to design a high Reynolds number, long endurance airfoil.

The long endurance time required an airfoil design with the following characteristics:

- o High lift (preferably without any flap deflection)
- o Low drag
- o Laminar flow to greatest extent possible (to minimize aircraft size)
- o Reasonable stall characteristics

Furthermore, it was desired to advance beyond the empirical approach to airfoil selection, that is, modifying a base airfoil with trial and error redesigning in the wind tunnel. This study utilized Boeing-developed inverse boundary-layer solution and inverse airfoil design computer codes to create an airfoil section that would achieve the performance goals and still have reasonable off design performance.

LONG ENDURANCE CPA DESIGN
(CONTINUOUS PATROL AIRCRAFT)

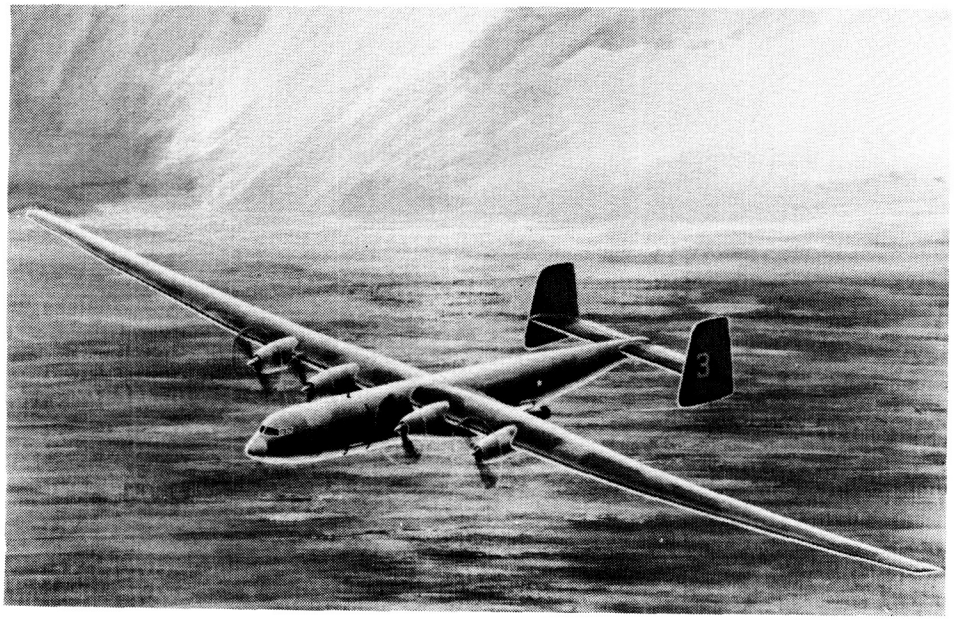

Figure 1.

INTRODUCTION (CONCLUDED)

Because the IR&D study was conducted in parallel with the CPA Program, most of the geometric and performance specifications for the 2-D airfoil reflect CPA mission specifications and requirements. As background for understanding the unusual design conditions, the following fundamental specifications were used from the CPA project:

- o Aspect Ratio: 21.6
- o Wing Area: 6000 ft^2
- o Span: 360 ft
- o Loiter Altitude: 5,000 ft
- o 145 kt endurance speed
- o Engine(s) type: turboprop

Figure 2 illustrates the high aspect ratio wing planform used for the CPA configuration and the design span loading for this wing geometry. This design study chose to formulate an airfoil for an outboard wing section (η=0.80) since this station represented the maximum required lift coefficient, and therefore was the critical airfoil for this loiter-design wing. The span loading curve integrates to a total airplane lift coefficient of 1.3.

WING PLANFORM AND SPANWISE LOADING

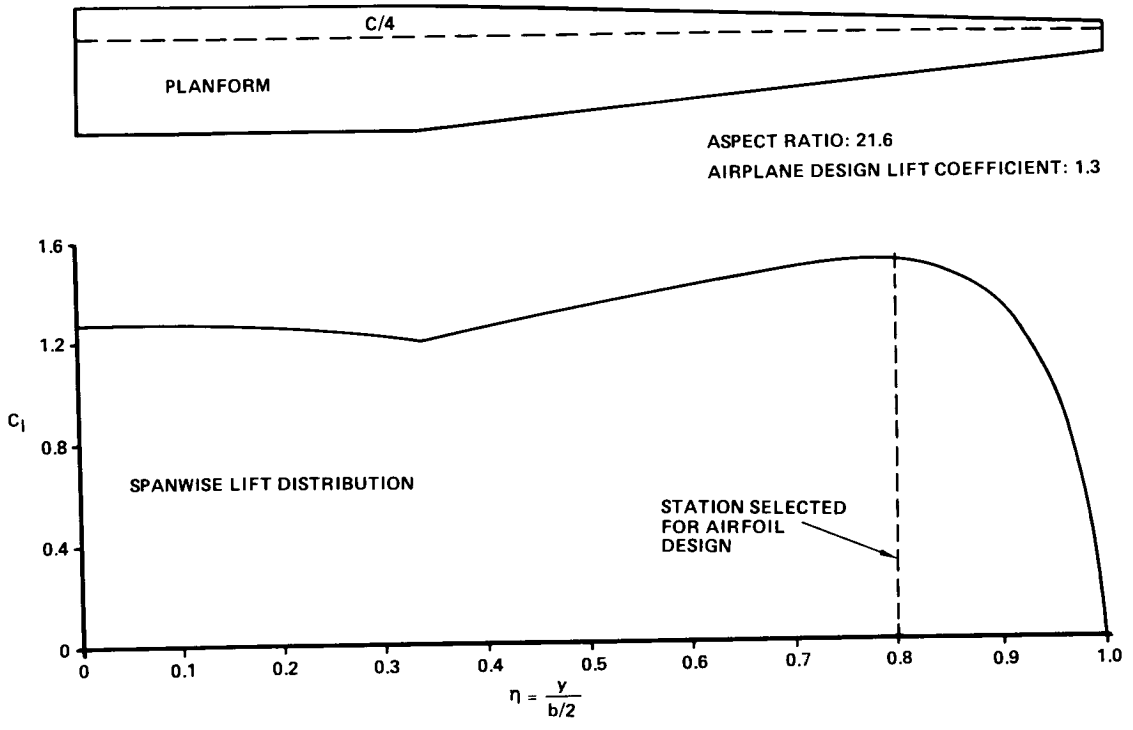

Figure 2.

AIRFOIL DESIGN REQUIREMENTS

Aspect Ratio and minimum drag coefficient (C_{Do}) are well-known to have a significant effect on both the endurance parameter $(C_L^{3/2}/C_D)_{MAX}$ and the lift coefficient at which the maximum endurance parameter is reached. The endurance improvement and the important reduction in lift coefficient with extent of laminar flow as shown in Figure 3, provided an impetus for obtaining as much laminar flow on the wing as possible.

DESIGN LIFT COEFFICIENT FOR ENDURANCE

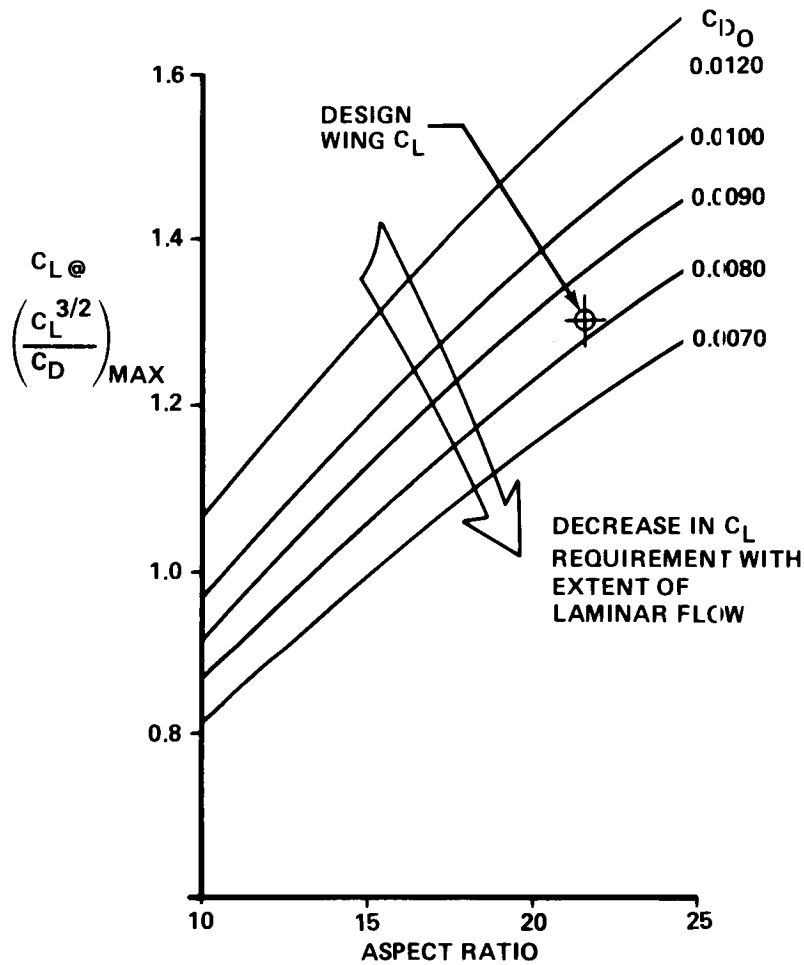

Figure 3.

Based on the CPA design specifications, airfoil design criteria were selected. These are listed in Figure 4. A total airplane lift coefficient of 1.3 resulted in section design and maximum lift coefficients of 1.5 and 2.2 respectively at the aforementioned outboard wing station. These values will produce a 20 percent stall margin. Well into the design phase it became evident that these section coefficients were difficult to attain. Thus, a revision to section design and maximum lift coefficients of 1.4 and 2.0 was established as a more approachable goal.

A design goal to maximize the extent of laminar flow resulted in developing an airfoil which would sustain natural laminar flow from L.E. to T.E. on the lower surface and from L.E. to 0.3c on the upper surface. The upper surface extent was largely dictated by the chord distance required for velocity deceleration and pressure recovery.

The low endurance speed requirement in combination with a 5000 ft loiter altitude, resulted in a design Mach number of 0.22. This low Mach number enabled a large thickness ratio (18%) to be used in meeting the high design lift coefficient requirement.

AIRFOIL DESIGN CRITERIA

- DESIGN C_l=1.4
- MAXIMUM C_l=2.0
- MAXIMUM THICKNESS = 0.18 C
- RN=14 x 10^6
- MACH NO. = 0.22
- LAMINAR FLOW, UPPER SURFACE, L.E. TO 0.3 C
- LAMINAR FLOW, LOWER SURFACE, L.E. TO T.E.
- NO UPPER SURFACE SEPARATION
- REASONABLE STALL CHARACTERISTICS (NON-ABRUPT)
- REASONABLE OFF-DESIGN PERFORMANCE

Figure 4.

AIRFOIL DESIGN PROCESS

The airfoil was designed through a "synthesis" or inverse design process developed by Boeing. The process utilizes inverse boundary-layer solution and inverse airfoil design computer codes to create an airfoil section which can attain specified characteristics and achieve reasonable off-design performance. This method, briefly described herein, is described more comprehensively in Reference 1 along with a discussion of the background of the computer codes.

The design process begins with the inverse boundary-layer solution where desired boundary-layer characteristics, performance objectives, and constraints are specified. Through the synthesis process a corresponding viscous flow pressure distribution is developed and an airfoil shape is extracted that meets the specified requirements. Current computer codes used by Boeing to accomplish the two inverse solution processes are:

A427 — for airfoil pressure distribution design and parametric studies

A456 — for detailed geometry design and final performance evaluation (including the effects of separated flow)

The A427 program has the capability to generate a pressure distribution and corresponding "seed" airfoil given a set of boundary-layer characteristics, performance goals, and physical constraints. (Figure 5.)

- DEFINE AIRFOIL SPECIFICATIONS (X_r/C, T.E. C_p, ETC)
- SPECIFY BOUNDARY-LAYER H IN RECOVERY REGION
- DESIGN PRESSURE DISTRIBUTION USING INVERSE BOUNDARY-LAYER THEORY (A427)
- EXTRACT SEED AIRFOIL

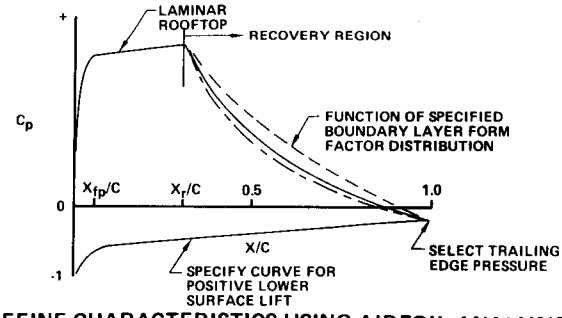

- REFINE CHARACTERISTICS USING AIRFOIL ANALYSIS AND DESIGN CODE (A456)
- EXTRACT FINAL AIRFOIL GEOMETRY (A456)

Figure 5.

AIRFOIL DESIGN PROCESS (CONCLUDED)

The Subsonic Airfoil Section System (A456) program is a general purpose 2-D, airfoil section analysis and design program. In the analysis mode the single element airfoil forces, moments, and boundary-layer characteristics are calculated at various angle of attack and flow conditions. Through the use of potential flow theory, boundary-layer theory, and separated flow modeling theory, the airfoil performance was predicted up to and beyond maximum lift. In the design mode the airfoil was reshaped to produce a desired pressure distribution.

Significant tasks involved in the iterative process of designing the airfoil are summarized in Figure 5. An important program input for designing the pressure recovery region is the boundary-layer form factor (H) distribution. Code A427 contains three forms of H distributions: a constant H, linear-increasing H, and exponentially increasing H. A linear-increasing H was selected to both maximize lift and soften the stall away from the sharp Stratford-type separation produced with a constant H distribution.

At the culmination of the design phase, an airfoil had been designed that analytically satisfied the required performance, achieved approximately 30 percent laminar flow on the upper surface, and was structurally practical. Figure 6 presents the airfoil contour and shows the amount of camber designed into the profile. This design phase was followed by a joint testing-verification effort between Boeing and NASA in which Boeing provided the 2-D airfoil and NASA contributed wind tunnel time and personnel at the Langley Low Turbulence Pressure Tunnel (LTPT).

GENERAL AIRFOIL CONTOUR

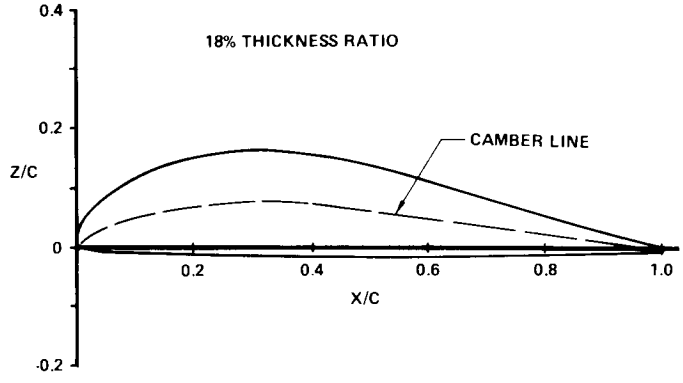

Figure 6.

TWO-DIMENSIONAL AIRFOIL MODEL

A solid aluminum airfoil section was built for testing in the NASA-Langley 2-D Low Turbulence Pressure Tunnel (LTPT). The installed model, shown in Figure 7, had a 32.0" chord and 36.0" span with a maximum thickness of 18 percent chord. The airfoil chord length was essentially limited by the largest length which could be physically accommodated on the end plates. It was recognized that the 32.0" chord would result in a high RN/ft at the design Reynolds number of 14×10^6. A 0.127c plain flap was built with options for three angular settings (excluding the nested position). Contour tolerances were kept to $\pm$.003" from the leading edge back to 0.75c and $\pm$0.006" from 0.75c to the trailing edge. A surface finish of 32 or better was specified. Surface waviness in the chordwise direction was to be no greater than 0.006" in 20". To prevent introducing flow disturbances, the airfoil was constructed with a minimum of joints or similar discontinuities. Figure 8 shows the two instrumentation cavities machined into the airfoil from the lower surface and the thick web retained to ensure structural rigidity. A thick flush contoured cover plate was fitted for bolting into a lower surface recess surrounding the two cavities. This cover plate and flap cove edges were the only visible surface discontinuities. These mating pieces were manufactured with special precautions to maintain the smoothest continuous contour possible. A tang at each end of the model was used to attach cirular end plates, which form part of the test section side walls, and in turn, flush mount the model on the left and right hand rotating inner drums of the pitching mechanism.

LTPT TEST 303-W3 AIRFOIL

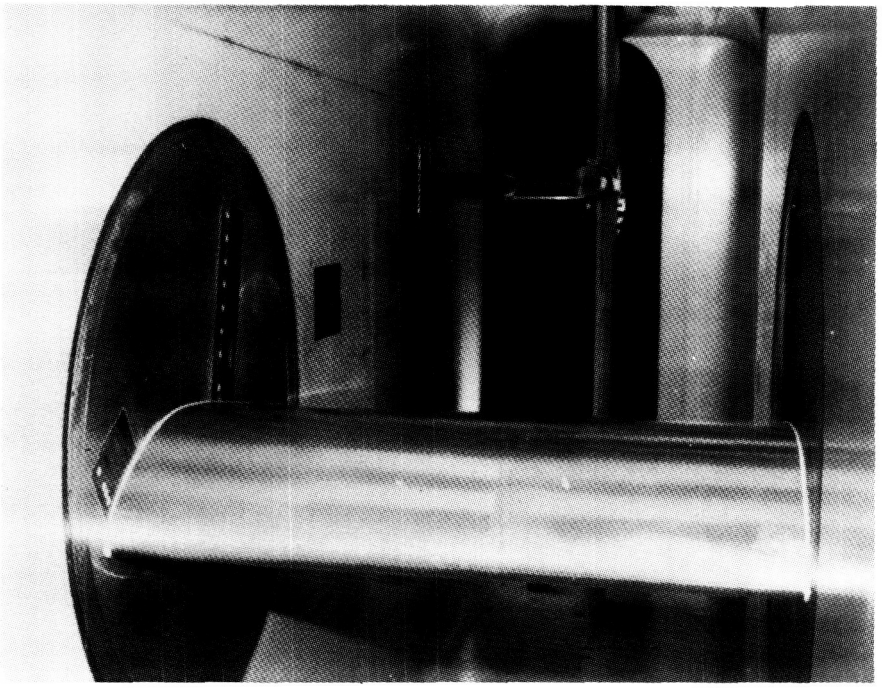

Figure 7.

MODEL VIEW SHOWING UNDERSURFACE
INSTRUMENTATION CAVITIES

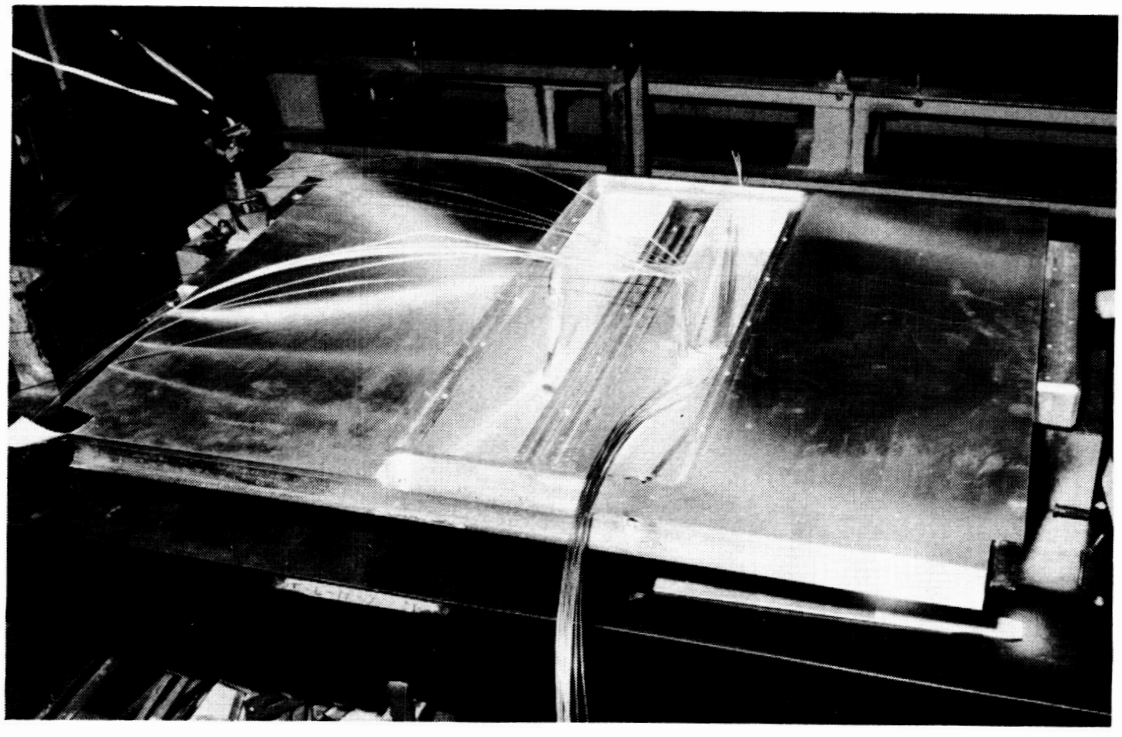

Figure 8.

INSTRUMENTATION

Pressure sensing instrumentation consisted of 53 static pressure orifices at one spanwise station: 32 on the upper surface and 21 on the lower surface. A slanted orifice pattern forward of 0.40c as shown in Figure 9 was utilized to preserve a smooth surface leading up to each forward orifice.

Flush mounted hot-film gages were used as boundary layer laminar-to-turbulent transition detection devices. By monitoring the root mean square (RMS) voltage of each hot-film sensor, in the natural or forced boundary-layer transition area of the upper surface, an indication of laminar flow, transition, or turbulent flow could be determined. Three types of output results were obtained for this test. First, a table of RMS voltage for each gage at each angle of attack was recorded. Second, this table was converted to integers of 1 to 4 representing the various boundary-layer stages from complete laminar through transition to full turbulent flow. Lastly, a plot of RMS voltage versus angle of attack for each gage was drawn giving an overall record of how a specific location changed from laminar to turbulent as angle of attack was increased. Ten hot-film gages were mounted flush in a slanted spanwise station pattern, covering the area from 0.17c to 0.44c on the upper airfoil surface, as illustrated in Figure 9.

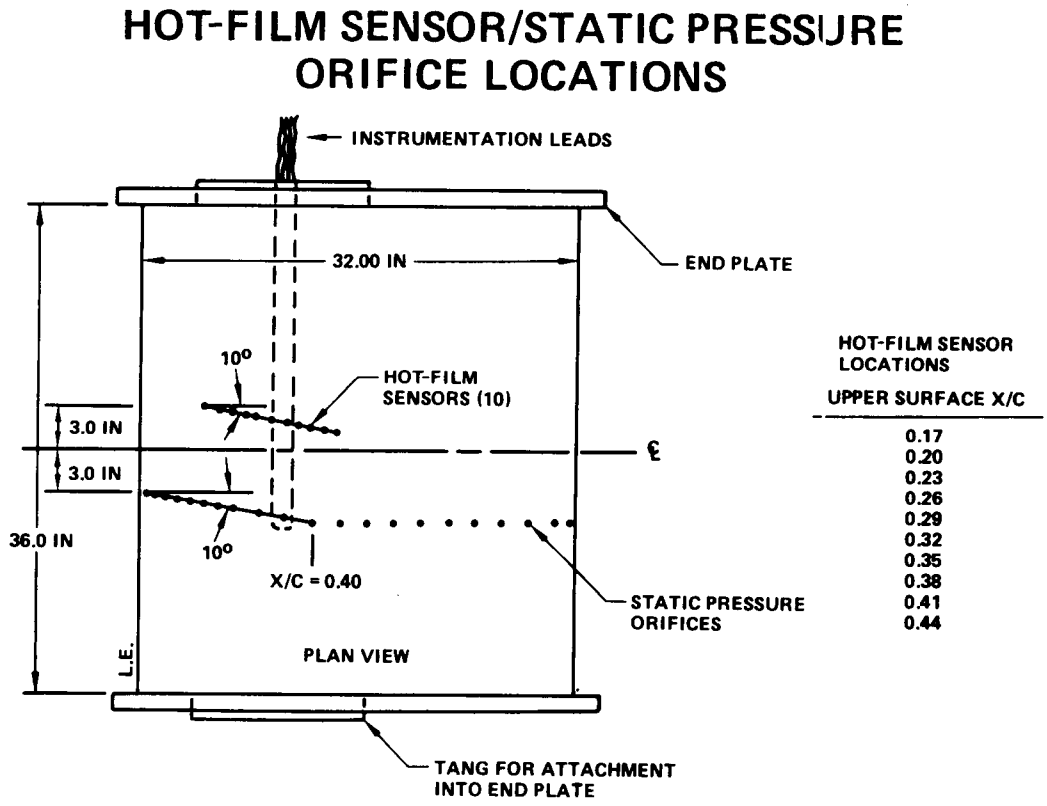

Figure 9.

TEST FACILITY

Two dimensional wind tunnel testing of the high lift/natural laminar airfoil was conducted at the NASA-Langley 3 ft x 7.5 Low Turbulence Pressure Tunnel (LTPT). This tunnel is designed to operate over a range of tunnel pressures from 160 psia to less than 1 psia, thereby providing full scale Reynolds number testing capability. The 2000 HP drive motor provides a speed capability of 0.46 Mach at 1 atm to 0.25 Mach at approximately a tunnel pressure of 120 psia.

Besides standard tunnel parameter values (Reynolds number, Mach number, angle of attack, etc.) data in coefficient form (C_l, C_d, and C_m) were obtained within an hour of completing a test run with the tunnel's data acquisition and data reduction system. Section lift coefficient was calculated by integrating the pressure measurements from the 53 static orifices located around the airfoil at one spanwise station. Section pitching moment coefficient was determined by summing the moments produced by the various measured static pressures about the 0.25c location.

Section drag coefficient was calculated from wake rake total pressure measurements. At each angle of attack, the sting mounted/remotely controlled/multi-probe rake was moved completely through the airfoil's wake. Drag profile plots showing the variation of drag coefficient with height as measured by each of the seven total pressure probes were obtained on-line. Section drag coefficient was calculated by integrating each of the drag profiles and then averaging. A limitation of the wake rake system was reached when the rake's traversing capability was exceeded by a wake depth expanded greatly by stall-generated flow separation. High loads due to turbulence intensity in a wake with airfoil flow separation at high static pressures was a second limitation. These drag measurement limitations prevented drag data acquisition at angles of attack beyond initial stall. The tunnel wake rake is visible in Figure 7.

CHORDWISE PRESSURE DISTRIBUTION

The theoretical chordwise pressure distributions selected to achieve the prescribed extent of natural laminar flow at the design section lift coefficient and Reynolds number of 1.4 and 14 x 10^6, respectively, is presented in Figure 10. The upper surface can be divided into four flow regions: 1. An acceleration region transisting into 2. A laminar roof with accelerating flow at the design conditions, 3. A forced transition region between 0.26 and 0.30c, and 4. A turbulent recovery region extending from 0.30c to the trailing edge. Note that a partial stagnation pressure recovery of about 0.25Cp was designed into the trailing edge area. The entire lower surface was designed to produce positive pressures to assist in achieving the high design lift coefficient. A continual flow acceleration is maintained from the leading edge to about 0.90c to aid in sustaining laminar flow. Figure 10 shows a close agreement over the entire upper and lower surface between theory and test data. However, theory does predict somewhat more positive pressure on the lower surface than was achieved.

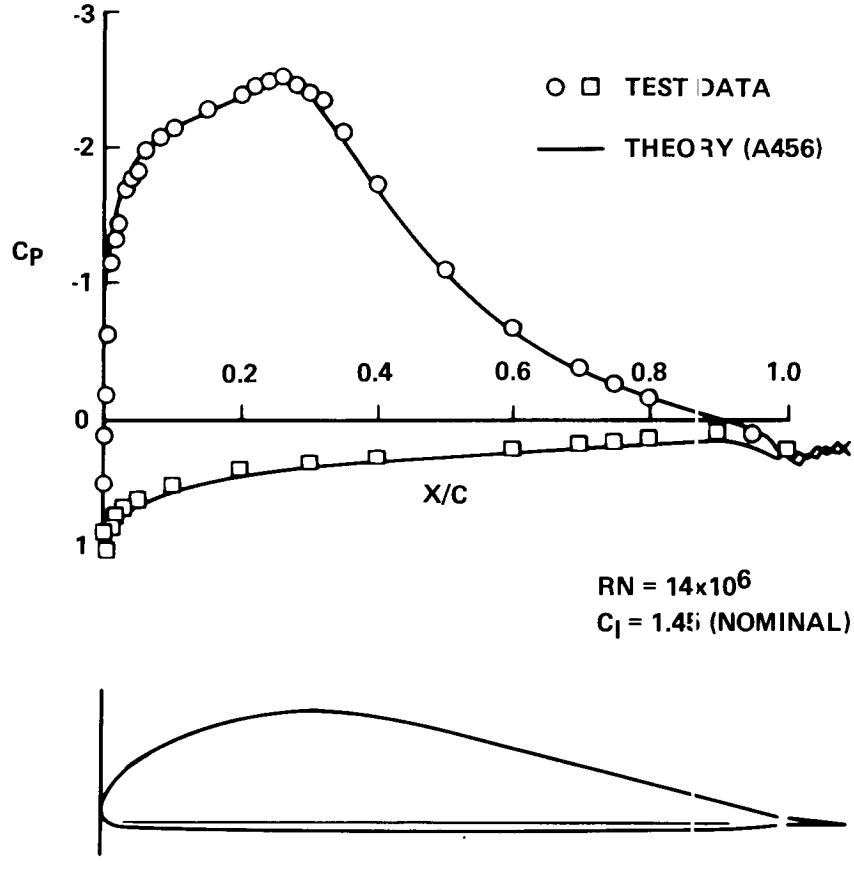

Figure 10.

CHORDWISE PRESSURE DISTRIBUTION (CONCLUDED)

One airfoil design criterion was reasonable off-design performance. Figure 11 presents three chordwise pressure distributions descending in lift coefficient from the design case at maximum endurance. That this goal was achieved in the lift component can be seen by noting the regular change in both upper and lower surface pressure coefficient over the entire chord (figure 11).

Also note that a deceleration zone is present near the lower surface leading edge at $0.94C_l$. This characteristic along with a flat pressure coefficient over the lower surface is not favorable for maintaining laminar flow. This situation will become more unfavorable for laminar flow on the lower surface at smaller lift coefficients.

OFF-DESIGN PRESSURE DISTRIBUTIONS

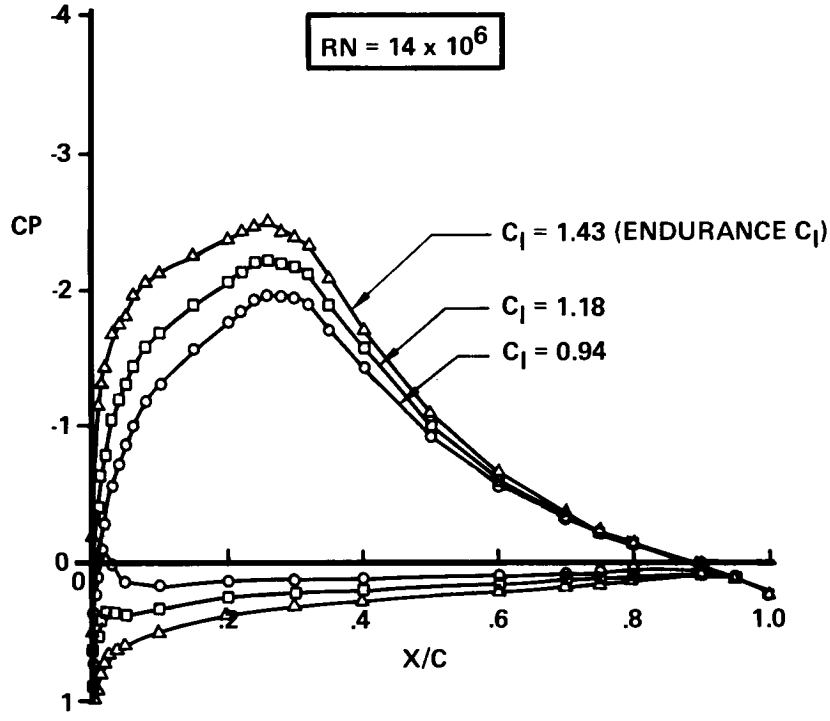

Figure 11.

BOUNDARY-LAYER ANALYSIS

The ten hot-film sensors installed in the upper surface from 0.17c to 0.44c were continuously monitored on scopes for signal content and permanent records were acquired, such as the two presented in Figure 12 where RMS voltage has been plotted as a function of angle of attack. Laminar flow is characterized by an almost zero RMS voltage. Transition is registered as a sharp rise in RMS voltage, a peak, and then a sharp decrease to a level indicative of fully turbulent flow. During the initial part of transition, the signal exhibits a laminar RMS voltage level mixed with bursts; in the second part the signal indicates turbulent flow mixed with bursts.

Prior to this test, experience level in using hot-film sensors as transition detectors was quite low. There was concern about sensor reliability, primarily due to their small size and fine wire leads. However, during the test this instrumentation was found to be trouble-free and rugged. If this had been known prior to the test, the lower surface would also have been instrumented.

HOT-FILM RESULTS

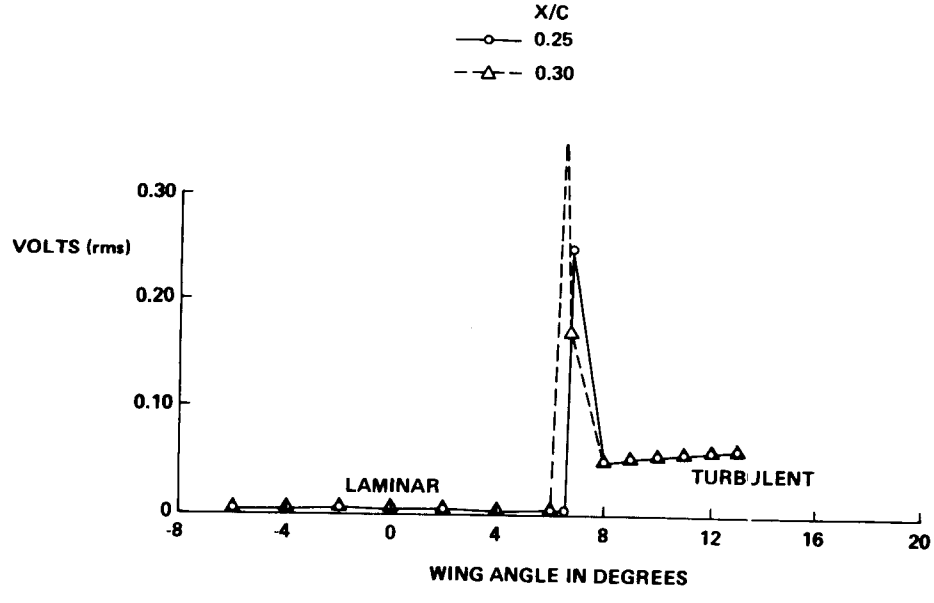

Figure 12.

Figure 13 presents hot-film data showing boundary-layer conditions as a function of chord during alpha sweeps at 14×10^6 and 12×10^6 Reynolds number. The data have been interpreted to establish chordwise extent of laminar flow and transition to fully developed turbulent flow. Note that the goal of obtaining laminar flow over the forward 30 percent chord was achieved. At 14×10^6 RN, the hot-film sensors indicated transition forward movement at 5.3^o alpha, an angle lower than predicted by theory. Transition forward movement was progressively delayed to higher alphas with decreasing Reynolds number. At 12×10^6 RN, Figure 13 shows that this movement occurs at 6.5^o alpha; at 10×10^6 RN, it is delayed to 10.5^o alpha.

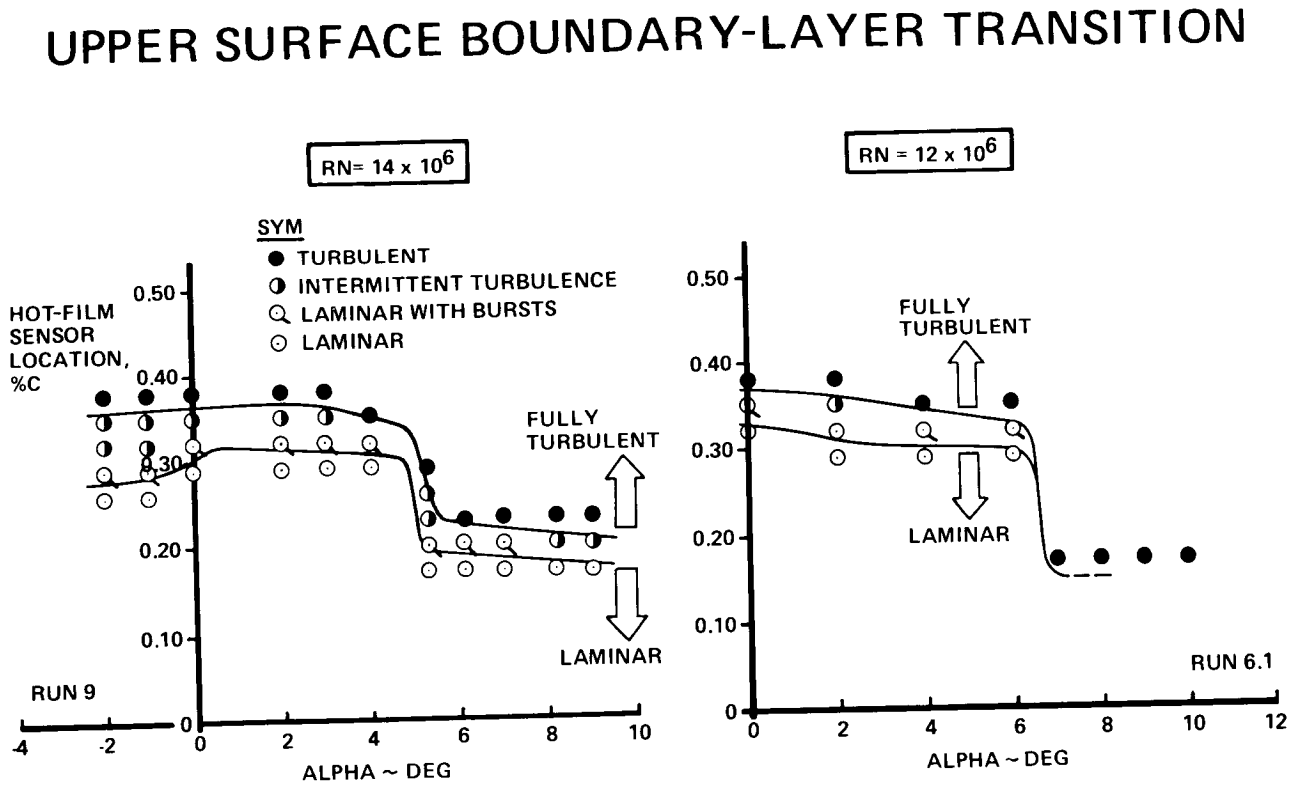

Figure 13.

REYNOLDS NUMBER EFFECTS

Figure 14 presents four lift curves obtained over a range of Reynolds numbers from $5x10^6$ to $14x10^6$. Note that whereas three of the pitch sweeps were performed close to the design Mach number of 0.22, the sweep for $14x10^6$ RN was conducted at 0.09 Mach. This deviation was caused by the practical necessity of relaxing the desired test Mach number to reduce tunnel pressurization pumping time.

Two characteristics of the lift curve can be observed: the decrease in lift curve slope with increasing Reynolds number and the decrease in maximum lift with increasing RN. An examination of chordwise pressure plots at 8^o alpha revealed higher negative pressure coefficients on the upper surface over the aft 80 percent chord at successively lower Reynolds number. At each test Reynolds number the stall was abrupt.

Measurement of an accurate maximum lift in a 2-D tunnel is a recognized problem due to boundary layer on the tunnel walls. During initial test runs, the impact of wall slot blowing using two blowing slots built into the model end plates (one forward and the second at 0.60c) was examined. Blowing did clean up initial flow separation in the corners between the aft wing surface and tunnel side walls, but only increased stall angle by 0.7^o before stall occurred evenly across the span. Since blowing only provided a modest improvement in stall angle and did not reduce stall abruptness, a decision was made to leave out slot blowing to materially reduce test time.

REYNOLDS NUMBER EFFECT ON LIFT CURVE

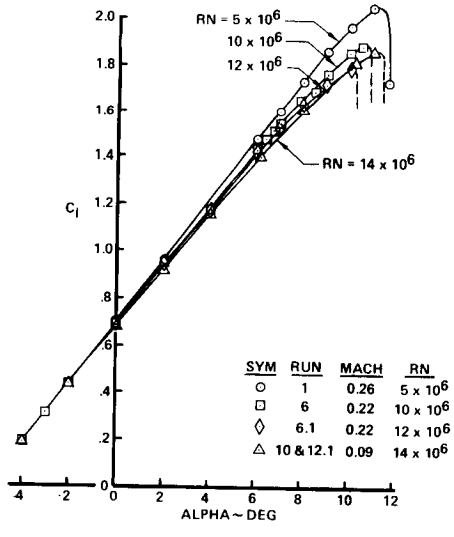

Figure 14.

Figure 15 presents the companion drag polars to the Figure 14 lift curves. The polars generally exhibit a flat drag over a range of lift coefficients from endurance levels down to the lowest test values, which is indicative of satisfactory off-design performance. Note the increase in drag at endurance level lift coefficients of 1.48 with 12×10^6 Reynolds number, for example. The departure in polar shape coincides with the forward movement in upper surface boundary-layer transition previously shown in Figure 13. At 4^o alpha, the drag level for both 10×10^6 and 12×10^6 RN curves closely match theory which includes laminar flow over the initial 30 percent of the upper surface and over almost the entire lower surface. The drag increase at 14×10^6 RN was a concern because it suggested premature transition on the lower surface.

REYNOLDS NUMBER EFFECT ON DRAG POLAR

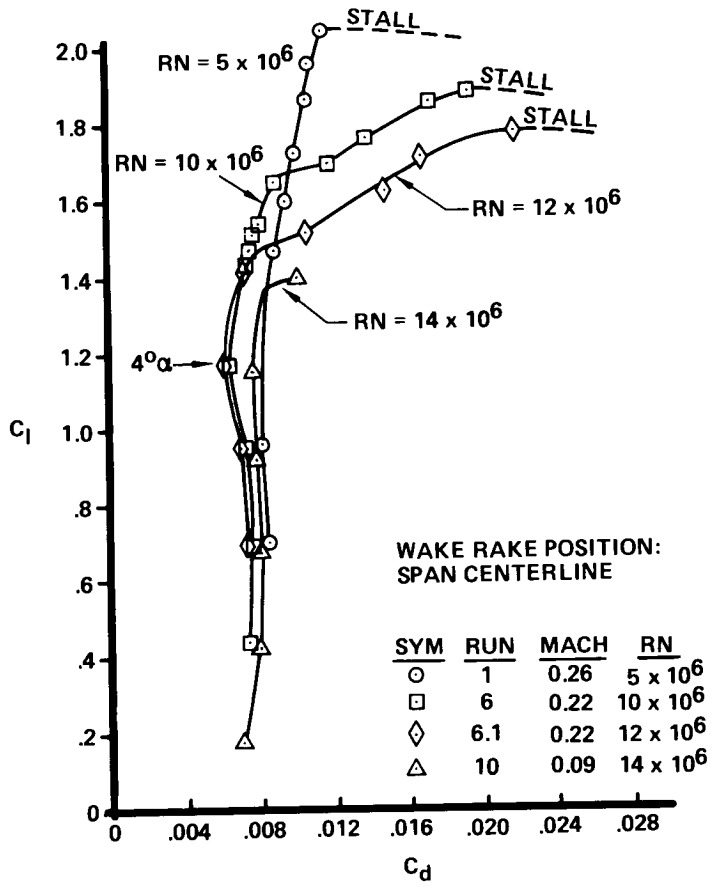

Figure 15.

LIFT AND DRAG COMPARISON WITH THEORY

The importance of properly locating instrumentation, and the care that must be taken in testing laminar-flow airfoils is illustrated in Figure 16. Two runs, increasing Reynolds number at a constant alpha of 4°, were performed to investigate the unexpected high drag at 14×10^6 RN and to obtain data for comparisons with theory. Upon examining the model it was observed that the wake rake was positioned behind the lower surface instrumentation cover plate during rake traverses. It was postulated that the access door with its edges and filled bolt head holes could trigger a premature transition on the lower surface. During the two RN runs, the wake rake was positioned at two different spanwise locations: behind the access door at the span centerline and the right hand side. Results presented in Figure 16 show two levels of drag. The lower drag level agrees with theory which includes the design goal of laminar-flow extent. The higher drag level, measured behind the access door, is consistent with a premise of turbulent flow being present over the entire lower surface. Test data shows that laminar-flow design goal could be maintained up to a Reynolds number of 18×10^6 at an alpha of 4°.

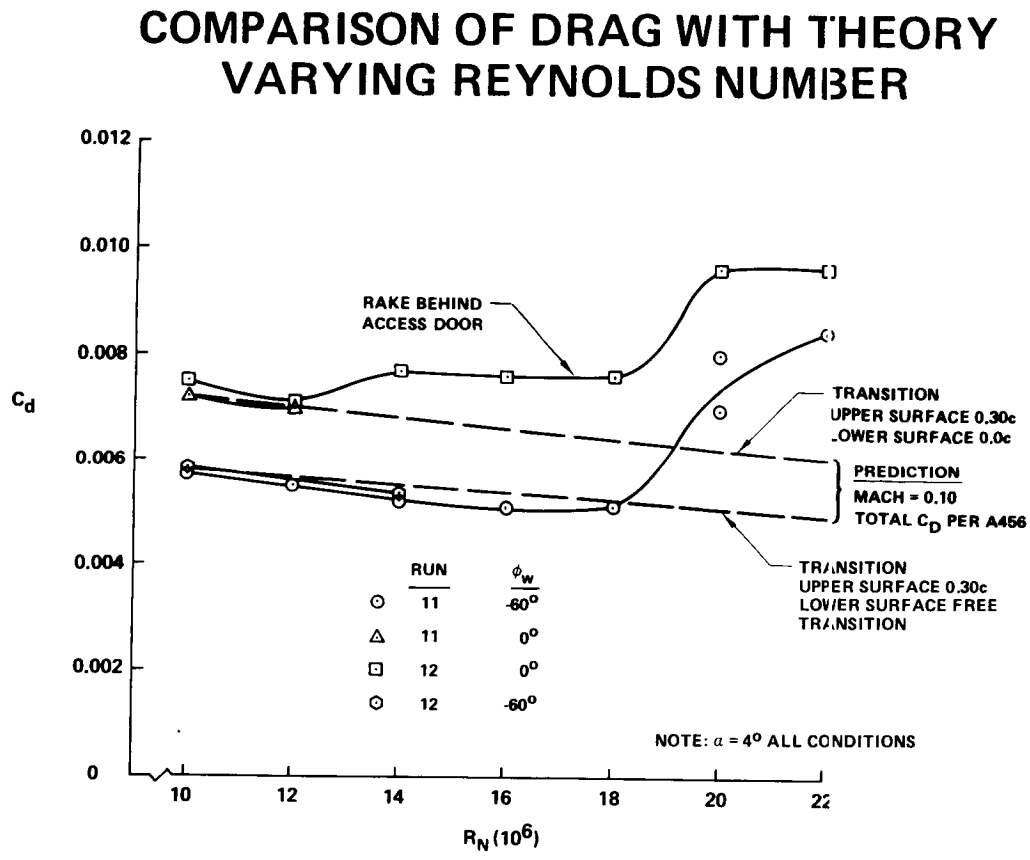

Figure 16.

The variation of drag with angle of attack at 14×10^6 Reynolds number, presented in Figure 17, shows that drag measured on the right hand side of the model (and not behind the access door) matches theory at angles of attack corresponding to endurance and cruise lift coefficients. A moderate drag increase above theoretical values occurred at 0° to 2° alpha. The increase is probably a result of pressure gradients developing on the lower surface that are unfavorable for sustaining laminar flow. This possibility was previously noted in discussing Figure 11 which presented off-design chordwise pressure distributions.

The drag departure from theory at 7^o alpha, which should include a drag increment from upper surface transition forward movement, is in conflict with hot-film data presented in Figure 13 and shows transition forward movement occurring at 5.3^o alpha. A question has been raised as to the validity of hot film sensors when they are used to detect boundary-layer transition at large values of Reynolds number per foot. The problem is that physical imperfections in the sensor installation could produce erroneous signals.

Data obtained from a trip strips-on run have also been plotted in Figure 17 to provide a reference for the drag levels achieved with natural laminar flow. These trip strips, installed at .025c upper surface and .035c lower surface were a dot-type configuration with a thickness determined to be only sufficient for tripping the boundary-layer at 14×10^6 Reynolds number. This was verified by comparing measured and predicted drag values.

COMPARISON OF DRAG POLAR WITH THEORY

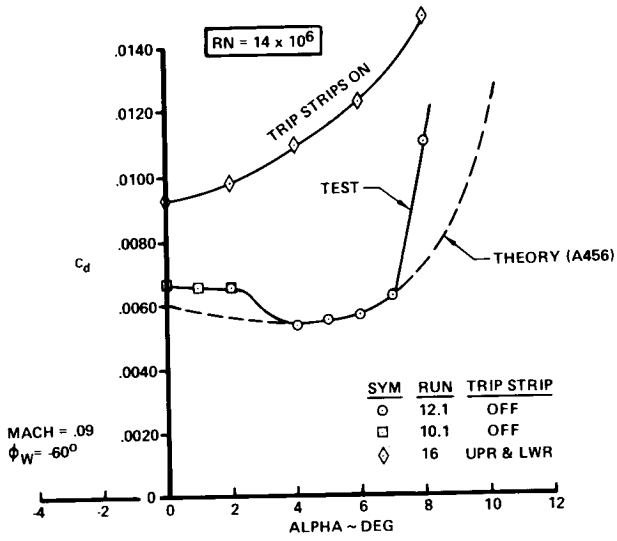

Figure 17.

LIFT AND DRAG COMPARISON WITH THEORY (CONCLUDED)

The lift curve acquired at 14×10^6 Reynolds number and 0.09 Mach number is presented in Figure 18 and compared with theory. There is some small deviation from theory in both angle for zero lift and lift curve slope; however, the most significant difference between theory and test is the stall region. Whereas theory predicted a maximum lift coefficient of 2.0 and a gradual stall with flow separation gradually progressing forward from the trailing edge, test data shows a lower maximum lift and a sharp stall. This stall characteristic is illustrated in Figure 19 which presents pre- and post-stall pressure distributions obtained at 14×10^6 Reynolds number. In 0.4^o of alpha, the airfoil stalled and separated flow has encompassed the aft 60 percent of chord. Peak pressures over the forward portion of the airfoil have decreased by 27 percent. Obviously, the airfoil design method did not incorporate the correct turbulent flow separation mechanism including wake modeling and/or did not correctly mathematically model the flow condition at the trailing edge. Consequently, the linear boundary-layer H distribution used in the pressure recovery region aft of 30 percent chord did not provide the desired soft stall for the highly cambered 18 percent thick section.

COMPARISON OF LIFT CURVE WITH THEORY

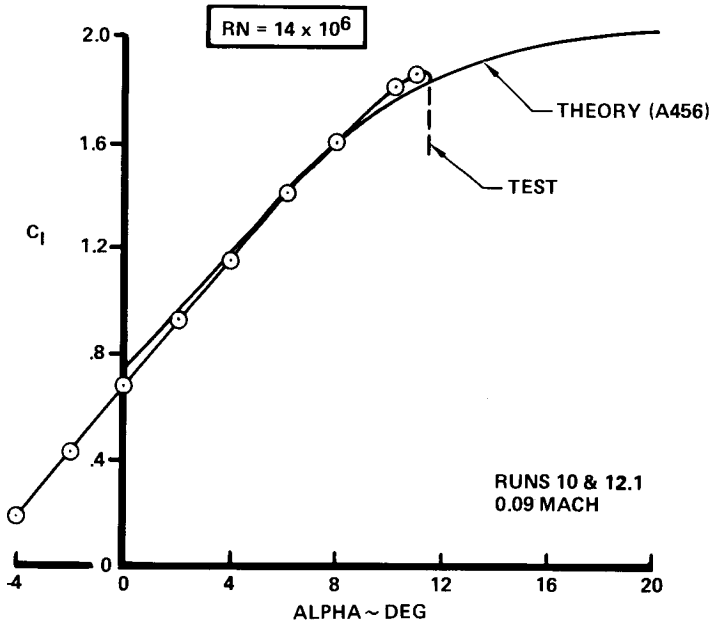

Figure 18.

CHORDWISE PRESSURE DISTRIBUTIONS: PRE-AND POST-STALL

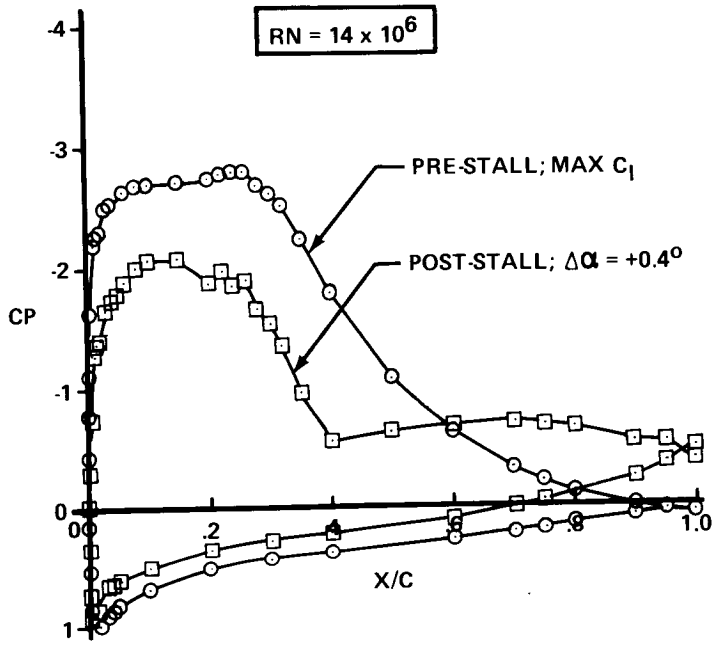

Figure 19.

LOW TRAILING EDGE FLAP DEFLECTION

A small 12.7 percent chord plain flap operating at low settings was proposed as a means of providing additional stall margin and modifying the wing stall pattern while incurring only a small drag penalty at cruise lift coefficients. The flap was designed to minimize contour deviations at both upper and lower flap cove trailing edges. The resultant small cavities were filled in for the zero flap angle testing. Figure 20 presents a comparison of flaps up and 5° flap data for 14x10 Reynolds number. The lift curves show the flap produces a consistent lift increment, varying from 0.21 ΔC_l at 0° alpha to 0.12 ΔC_l at stall. The maximum lift coefficient of 2.0 matches the design goal; however, the stall character did not deviate from the sharp stall recorded by the flaps up configuration.

Figure 20 also shows that the drag polar obtained with 5° of flap deflection exhibits only a small variation in drag from the lowest angle of attack tested up to the design lift coefficient of 1.4. At this lift coefficient, the drag increment for the flap is 15 drag counts, which is attributed to a reduction in laminar flow on the lower surface. This reasoning followed an examination of hot-film sensor data. At $1.4C_l$ transition to turbulent flow occurred aft of 0.32c. Unlike data from flaps up runs, the 5° flap polar shows a smooth, continuous and non-abrupt drag variation from 1.5 C_l up to stall where a typical large drag increase occurred.

LIFT AND DRAG CHARACTERISTICS WITH 5° OF FLAP
RN = 14x10⁶

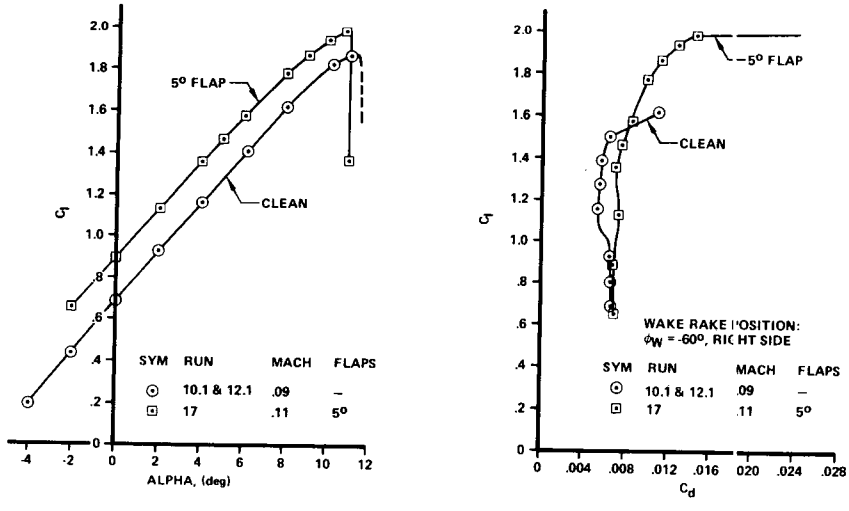

Figure 20.

CONCLUSIONS

Although limits of applicability of the design tools were pushed severely, the theoretically designed airfoil came very close to meeting the design goals. The predicted extent of natural laminar flow (over the forward 0.3c of the upper surface and over almost the entire lower surface) was obtained at the design goals of 1.4 C_l and 14×10^6 Reynolds number, good off-design airfoil performance was achieved at all tested lift coefficients below the endurance level, and a small plain flap at a low deflection can be used to improve stall margin for only a small drag penalty at cruise and endurance lift coefficients (Figure 21).

The major shortcoming of the computer codes was an inability to correctly model the stall character. Unlike theory that predicted a gradual stall with flow separation moving slowly forward from the trailing edge, test data showed a sharp stall with flow separation rapidly moving forward from the trailing edge up to 0.40c. This stall occurred at a lower than predicted stall angle, which resulted in a lower than predicted maximum lift coefficient. It is evident the current inverse airfoil design process does not mathematically model the correct flow separation mechanism for the type of thick airfoil tested. Additional airfoil analysis work is being performed with a revised A456 program, namely a modified wake-modeling procedure, to investigate stall predictions for the high camber/large thickness ratio class of airfoil. Data also showed that transition on the upper surface occurred earlier than predicted. The combination of a high design C_l and large Reynolds number did stretch the capability of the current airfoil design computer codes, and/or possibly the large test RN/ft created a problem.

- THE PREDICTED EXTENT OF NATURAL LAMINAR FLOW WAS ACHIEVED AT THE DESIGN GOALS OF 1.4 C_l AND 14×10^6 RN
- GOOD OFF-DESIGN AIRFOIL PERFORMANCE IS AVAILABLE OVER A WIDE RANGE OF LIFT COEFFICIENTS
- A SMALL PLAIN FLAP AT 5^o CAN IMPROVE STALL MARGIN WITHOUT INCURRING MORE THAN A SMALL ENDURANCE DRAG PENALTY
- THE AIRFOIL DESIGN PROCESS DID NOT CORRECTLY MODEL STALL CHARACTER

Figure 21.

REFERENCES

1. McMasters, John H., and Henderson, Michael L.: Some Recent Applications of High Lift Computational Methods at Boeing. Journal of Aircraft, Volume 20, No.1, January 1983.

ACKNOWLEDGMENTS

The author would like to thank Robert McGhee (NASA-Langley Research Center) for coordinating and conducting the test and then developing the test data, Victor R. Page (Boeing Military Airplane Company) for the majority of the airfoil design, and William M. Ralph (Boeing Military Airplane Company) for preparing the test report.